

# FHO-based Hybrid Neural Networks for Short-Term Load Forecasting in Economic Dispatch of Power Systems

Yi Wei

College of Computer Science and Mathematics,  
Fujian University of Technology, Fuzhou 350118, China  
923398284@qq.com

Chia-Hung Wang\*

<sup>1</sup>College of Computer Science and Mathematics,  
Fujian University of Technology, Fuzhou 350118, China  
<sup>2</sup>Fujian Provincial Key Laboratory of Big Data Mining and Applications,  
Fujian University of Technology, Fuzhou 350118, China  
jhwang728@hotmail.com

Yi-Fan Suo

College of Computer Science and Mathematics,  
Fujian University of Technology, Fuzhou 350118, China  
752396822@qq.com

Qi-Gen Zhao

College of Computer Science and Mathematics,  
Fujian University of Technology, Fuzhou 350118, China  
1098868632@qq.com

Jin-Chen Yuan

College of Computer Science and Mathematics,  
Fujian University of Technology, Fuzhou 350118, China  
395589963@qq.com

Shu-Meng Chen

College of Computer Science and Mathematics,  
Fujian University of Technology, Fuzhou 350118, China  
1615780452@qq.com

\*Corresponding author: Chia-Hung Wang  
Received May 6, 2023, revised March 13, 2024, accepted June 21, 2024.

**ABSTRACT.** *With the development of the smart grid era, the data volume of the power system on the user side is growing rapidly, and the dependence of citizens on electricity is increasing significantly. In this paper, we aim to maximize the benefits of both supply and demand in the power system, from two aspects: improving the accuracy of short-term load forecasting and optimizing the economic dispatch of the power system. Firstly, based on the analysis of electricity consumption data, an improved load forecasting method via hybrid neural network is proposed. After determining the prediction results of the proposed model, we solved a short-term economic dispatch problem with the objective function of minimizing the generation cost of the power system and constraints such as unit start-up and shutdown, to achieve optimization of economic dispatch. In this work, an improved hybrid neural network with Firehawk Optimization (FHO) algorithm is developed to improve the accuracy of the prediction model by optimizing hyperparameters such as input data, number of hidden layer neurons, and batch size. In a series of numerical experiments, the proposed method is compared with other well-known optimization algorithms, such as Particle Swarm Optimization (PSO), Grey Wolf Optimiser (GWO) and Wild Horse Optimisation (WHO). From the comparison results, it shows that our method achieves better performance evaluation, and also improves the prediction accuracy of neural network models. Based on the load forecasting results, we determine the optimal scheduling scheme for the combination of power supply units, which minimizes the load and achieves higher applicability.*

**Keywords:** electric power system; economic dispatch problem; firehawk optimization algorithm; supply and demand sides; electric load forecasting; smart power grids.

---

1. **Introduction.** In the face of growing electricity demand, the task of ensuring a smooth supply in the power industry is still heavy. Meanwhile, with the development of electric vehicles, big data and 5G [1, 2, 3, 4], the importance of electric energy in the energy field is becoming more and more prominent. Therefore, the demand for electric energy in people's life is becoming more and more important. Besides, the proportion of electric energy in the demand side is also gradually increasing, and the demand for electric energy in the whole society is becoming larger and larger. Hence, the task of the electric power system to guarantee the balance between supply and demand side is still heavy [5]. For example, it was predicted that the share of electric energy in end-use energy consumption will increase to about 35% by about Year 2035 [6].

The study of power load forecasting has a great role in the normal and economic operation of power systems [7]. The safe and stable economic operation of the power system is not only beneficial to the development of society, but also to optimize the allocation of resources and to relieve the increasingly tight energy pressure. One of the characteristics of electric energy is difficult to store, so the power sector needs to have a general judgment of the future load trend in order to make reasonable scheduling arrangements for electric energy so that the power system's generation, transmission, distribution, transformation and consumption processes can achieve a dynamic balance of supply and demand [8]. Power load forecasting is a key component of the smart grid, and its accuracy is crucial for the safe and stable operation and economic operation of the power system. In practice, power systems aim to maximize efficiency while satisfying the interests of both supply and demand, which is the ideal goal of power operators. Improving the accuracy of short-term load forecasting can help grid dispatching departments make more scientific and effective economic dispatching decisions to ensure safe and stable operation of the power system [9, 10].

With the development of big data and cloud computing technologies, load forecasting methods based on deep learning algorithms have been widely used [11]. Deep learning algorithms have powerful modeling ability and adaptiveness, can automatically extract

features from data, and can handle large-scale data. Several models in deep learning algorithms have become the mainstream methods in load forecasting [12, 13], such as Recurrent Neural Networks (RNN) [14] and Long Short-Term Memory (LSTM) neural networks [15]. In the literature [16], a multiple linear regression model was applied to classify demand-side loads into various types such as customer residential, commercial electricity, and factory electricity, and influencing factors such as temperature were selected as input parameters for model prediction, and experiments showed that the method outperformed the traditional multiple regression model. Sina and Kaur [17] applied Support Vector Regression (SVR) model for load forecasting, combined with a spider-seeking algorithm to find the optimal parameters of the SVR model, and the experimental results showed that the accuracy of the SVR model combined with the optimization algorithm was higher than that of the ordinary SVR forecasting model. Sajjad et al. [18] proposed a combined neural network-based prediction method with a model combining both Gating Neural Network (GRU) and Convolutional Neural Network (CNN), via extracting the CNN features in the dataset to input into the GRU, and their results showed that the combined model has better prediction accuracy than the simple model. In general, the development of load forecasting technology has undergone an evolutionary process from rules of thumb to statistical models and machine learning algorithms to neural networks and deep learning algorithms [19, 20, 21, 22]. With the continuous progress of technology, the accuracy and efficiency of load forecasting have been improved [10, 23], which is of great significance for the safe and stable operation of power systems and optimal allocation of resources.

Therefore, in this paper, a neural network algorithm is used for load prediction, but considering that the neural network model is complex and computationally intensive in setting and finding parameters. Meanwhile, the Fire Hawk Optimization (FHO) algorithm is introduced and compared with commonly used optimisation algorithms, such as Particle Swarm Optimisation (PSO), Grey Wolf Optimiser (GWO) and Wild Horse Optimisation (WHO). In our comparison experiments, it reveals that the FHO optimization algorithm has higher search speed and finding quality compared with other optimization algorithms. Then a hybrid prediction model based on FHO-LSTM is constructed to improve the accuracy of load prediction. Finally, based on the prediction results of the improved model, a short-term economic dispatch model is developed to optimize economic dispatch with the minimization of power system generation costs as the objective function and constraints such as unit start-ups and shut-downs.

The main contributions of this paper are summarized in the following:

- (1) In this paper, the neural network algorithm is used to predict the load, but considering that the neural network model is complex and computationally intensive in setting and finding parameters. Hence, the FHO algorithm is introduced in this work and compared with other commonly used optimization algorithms such as PSO, etc. The comparison shows that the FHO optimization algorithm has a higher search speed and finding quality than other optimization algorithms. The comparison shows that the FHO optimization algorithm has a higher search speed and finding quality than other optimization algorithms.
- (2) This paper constructs a hybrid prediction model based on FHO-LSTM, which combines the FHO optimization algorithm and neural network to improve the accuracy of the model by optimizing the input data, the number of neurons in the hidden layer, the batch size and other hyper-parameters. The experimental comparison with LSTM is carried out to explore the advantages of the model.

- (3) Based on the load forecasting method and the analysis of the forecasting results proposed in this paper, further research is carried out on the optimization of short-term economic dispatching decisions for power systems. Combined with the load forecasting results, an optimal dispatching model for unit combinations is proposed. Moreover, the effectiveness of the load forecasting method proposed in this paper in reducing the operating costs of power systems is verified through experimental simulations.

The rest of the paper is organized as follows. In Section 2, we introduce the economic dispatch for supply and demand sides in the electricity market. In Section 3, we propose an improved firehawk optimization algorithm, which will be compared with three algorithms (PSO, GWO, and WHO) through a series of numerical comparisons. Next, in Section 4, we will present an improved hybrid prediction model via the studied FHO algorithm, and introduce our experimental setup and numerical results. Based on the obtained forecasting results, we will determine an optimization scheme for the economic load dispatch problem in Section 5. Finally, in Section 6, we summarize the conclusions in this work and point out the possible application in the future work.

**2. Economic dispatch for supply and demand sides in power systems.** In the field of power system planning and operation, optimizing the economic operation of power systems is a very important topic [10, 24, 25, 26, 27]. This helps to develop more scientifically efficient economic dispatch decisions, thus ensuring the safe operation of the power system.

As shown in Figure 1, a conceptual diagram of today's smart grid is illustrated. A smart grid is an intelligent energy system based on advanced information and communication technologies. Its structure includes the following main components:

- Supply side: including various energy generation such as hydroelectric power plants, Nuclear power plants, and distributed power sources, e.g., wind power, photovoltaic, etc.
- Demand side: including the electricity consumption side of households, new energy vehicles, factories, etc. for consuming electricity.
- Information side: monitoring, analysis, prediction and control of power generation, transmission, distribution and use of the power system through technologies such as the Internet of Things, big data and artificial intelligence.
- Energy storage side: including various energy storage devices, such as the batteries and supercapacitors, for regulating the load balance of the power system and responding to emergencies.
- Grid control system: through the market mechanism, supply and demand are regulated to achieve a reasonable allocation of electricity.

These components are interconnected through information technology to achieve efficient operation and management of the power system. At the same time, the smart grid can also interact with other energy systems (such as water, gas and heat) to form a more integrated energy system. As shown in Figure 1, it points out the position of supply and demand sides in the smart grid, and it also shows the economic load dispatch problem in the electricity market considered in this paper. The left side of the diagram shows the supply side of the power system, including various energy plants. On the right side of the diagram is the demand side of the grid, including residential electricity, factory electricity, new energy vehicles, etc. With the application of electric vehicles and other facilities to the grid system in recent years, the magnitude and scope of the load-side response

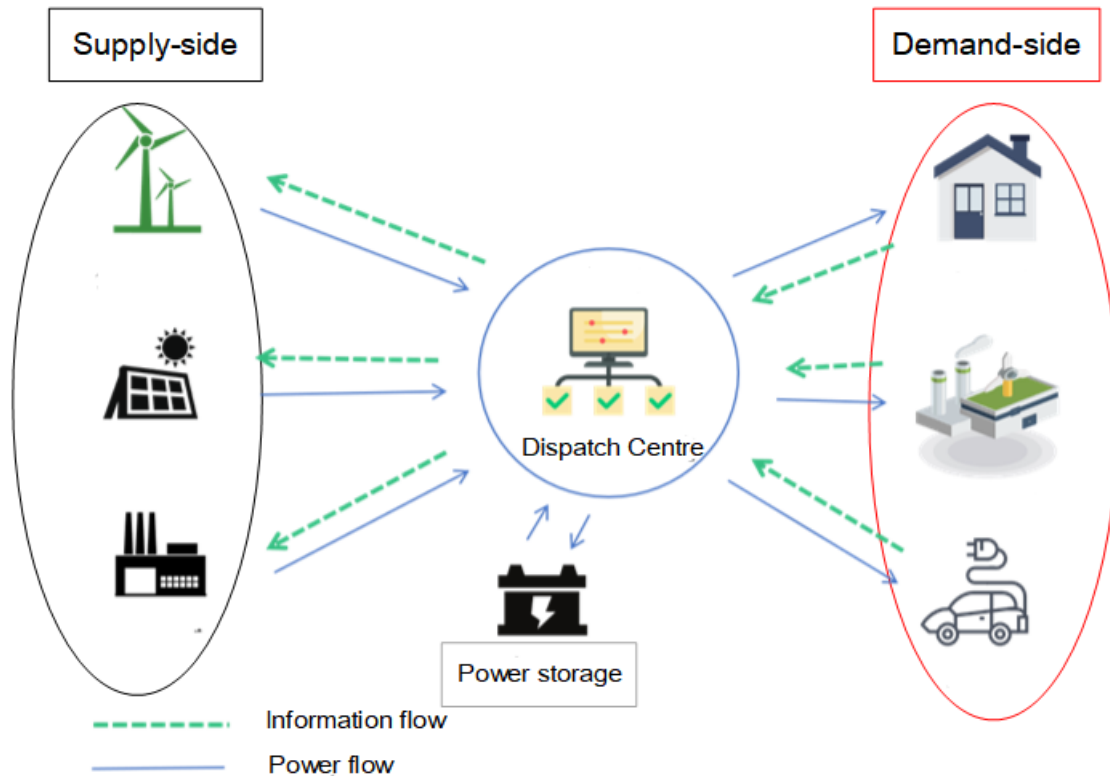


FIGURE 1. The concept diagram of supply and demand sides in the electric power system.

has been expanding, especially with the rapid growth of new energy loads, which has an important impact on the distribution grid load.

**3. An improved firehawk optimization algorithm.** In this section, we are going to introduce an improved hybrid neural network load forecasting method combined with the FHO algorithm. In order to improve the prediction accuracy of the studied neural network, we also compare the improved FHO algorithm with other algorithms [28]. By optimizing the input data and optimizing hyperparameters such as hidden layer size and batch size, the effect of improving the accuracy of the model can be achieved [29, 30, 31, 32, 33, 34]. Then, an improved model based on the combination of the FHO algorithm and neural networks is presented, and experiments are carried out to predict the electricity load data in areas A and B with LSTM and the corresponding improved algorithms respectively, and experimental results are obtained.

The Fire Hawk Optimizer [35] was developed as a metaheuristic algorithm based on the foraging behavior of brown falcons. The FHO algorithm simulates the foraging behavior of a firehawk, considering the setting and propagation of fire and the capture of prey. First, several candidate solutions ( $X$ ) are identified as position vectors for the firehawk and the prey. A random initialization process is used to identify the initial positions of these vectors in the search space.

$$X = \begin{bmatrix} X_1 \\ X_2 \\ \vdots \\ X_i \\ \vdots \\ X_N \end{bmatrix} = \begin{bmatrix} X_1 \\ X_2 \\ \vdots \\ X_i \\ \vdots \\ X_N \end{bmatrix} \begin{bmatrix} X_1^1 & \cdots & X_1^j & \cdots & X_1^N \\ \vdots & & \vdots & & \vdots \\ X_i^1 & & \cdots & & X_i^N \\ \vdots & & \vdots & & \vdots \\ X_d^1 & \cdots & X_d^j & \cdots & X_d^N \end{bmatrix}, \text{ for } i = 1, 2, \dots, N \text{ and } j = 1, 2, \dots, d, \tag{1}$$

$$x_i^j(0) = x_{i,\min}^j + rand.(x_{i,\max}^j - x_{i,\min}^j), \tag{2}$$

where the position of the current best individual is represented by  $position_{best}$ . Here,  $N$  is the total number of candidate solutions in the search space;  $x_i^j$  is the  $j$ -th decision variable of the  $i$ -th candidate solution;  $x_i^j(0)$  denotes the initial position of the candidate solution;  $x_{i,\min}^j$  and  $x_{i,\max}^j$  are the minimum and maximum bounds of the  $j$ -th decision variable of the  $i$ -th solution candidate; and  $rand$  is a uniformly distributed random number in the range of  $[0, 1]$ .

To determine the position of the firehawk in the search space, the objective function evaluation of the candidate solutions considers the chosen optimization problem. Some candidate solutions with better objective function values were denoted as firehawks, while the rest of the candidate solutions were prey. The selected firehawks are used to spread flames around the prey in the search space to make the hunt easier. In addition, the global best solution is assumed to be the primary fire used by the firehawk first in the search space. The mathematical representation is as follows:

$$PR = \begin{bmatrix} PR_1 \\ PR_2 \\ \vdots \\ PR_k \\ \vdots \\ PR_m \end{bmatrix}, \text{ for } k = 1, 2, \dots, m, \tag{3}$$

$$FH = \begin{bmatrix} FH_1 \\ FH_2 \\ \vdots \\ FH_p \\ \vdots \\ FH_n \end{bmatrix}, \text{ for } p = 1, 2, \dots, n, \tag{4}$$

where is the  $k$ -th prey in the search space with respect to the total number of  $m$  prey; considering the total number of  $n$  firehawks in the search space,  $FH_p$  is the  $p$ -th firehawk.

In the next stage of the studied FHO algorithm, the total distance between the firehawk and the prey is calculated. The closest prey to each bird is determined, thus distinguishing the effective territories of these birds. It is important to note that the prey closest to the first firehawk with the best objective function value is determined, while the territories of the other birds are considered through the remaining prey. Here,  $D_k^p$  is determined by the following equation:

$$D_k^p = \sqrt{(x_2 - x_1)^2 + (y_2 - y_1)^2}, \text{ for } p = 1, 2, \dots, n \text{ and } k = 1, 2, \dots, m, \tag{5}$$

where  $D_k^p$  is the total distance between the  $p$ -th firehawk and the  $k$ -th prey, and  $M$  is the total number of prey in the search space. The notation  $n$  is the total number of firehawks in the search space,  $(x_1, y_1)$  and  $(x_2, y_2)$  denote the coordinates of the firehawk and prey in the search space, respectively.

After the procedure described above for measuring the total distance between firehawk and prey, the territories of these birds are distinguished by the nearest prey around them. The search process of the algorithm is configured by classifying the firehawks and the prey. It is important to note that the firehawk with the better objective function value for its particular territory selects the best nearest prey in the search space. The other firehawks then complete the next closest prey in the search space.

In the next stage, the firehawks collect burning sticks from the main fire in order to set fire in the selected area. During this stage, each bird picks up a burning stick and drops it on its particular territory, forcing the prey to scurry away. At the same time, some birds desire to use burning sticks from other firehawk territories; therefore, these two behaviors can be used as a process of position updating in the main FHO search cycle, as shown in the following equation:

$$FH_p^{new} = FH_p + (r_1 \times GB - r_1 \times FH_{Near}), \text{ for } l = 1, 2, \dots, n, \quad (6)$$

where  $FH_p^{new}$  is the new position vector of the  $p$ -th firehawk. Here,  $GB$  is the global optimal solution in the search space, and is considered to be the main fire. Besides,  $FH_{Near}$  is another firehawk in the search space, and  $r_1$  and  $r_2$  are uniformly distributed random numbers in the range  $(0, 1)$  used to determine the movement of the firehawk towards the main fire position and other firehawk territory positions.

Next, the movement of prey within each firehawk's territory was considered a key aspect of animal behaviour for the location update process. When a firehawk throws a burning stick, the prey decides to hide, run away, or will make the mistake of running towards the firehawk. The following equation can be used to consider these movements during the location update process:

$$PR_q^{new} = PR_p + (r_3 \times FH_p - r_4 \times SP_p), \text{ for } p = 1, 2, \dots, n \text{ and } q = 1, 2, \dots, r, \quad (7)$$

where  $SP_p$  is the safe location under the territory of the  $p$ th group of firehawks;  $r_3$  and  $r_4$  are random numbers uniformly distributed in the range  $(0, 1)$  used to determine the movement of prey towards the firehawks and the safe location.

In addition, prey may move towards other firehawk territories, and in nearby ambushes, prey may move closer to the firehawk or even attempt to hide in safer locations outside of the firehawk territory. The following equation can be used to consider these movements during location updates:

$$PR_q^{new} = PR_p + (r_5 \times FH_{Alter} - r_6 \times SP_p), \begin{cases} p = 1, 2, \dots, n \\ q = 1, 2, \dots, r \end{cases} \quad (8)$$

where  $FH_{Alter}$  is another type of firehawk in the search space;  $r_5$  and  $r_6$  are random numbers uniformly distributed in the range  $(0, 1)$ , identifying the movement of prey towards other firehawks and safe places outside the territory.

Because of the reason that safe places in nature are places where most animals gather to stay safe from danger, the computations of  $SP_p$  and  $SP$  can be determined as follows:

$$SP_p = \frac{\sum_{q=p}^r PR_q}{r}, \text{ for } q = 1, 2, \dots, r \text{ and } p = 1, 2, \dots, n, \quad (9)$$

$$SP = \frac{\sum_{k=1}^m PR_k}{r} \text{ for } k = 1, 2, \dots, m, \quad (10)$$

where  $PR_k$  is the  $q$ -th prey surrounded by the  $q$ -th firehawk, and  $PR_k$  is the  $k$ -th prey in the search space. Ultimately, the algorithm flow chart is shown in Figure 2.

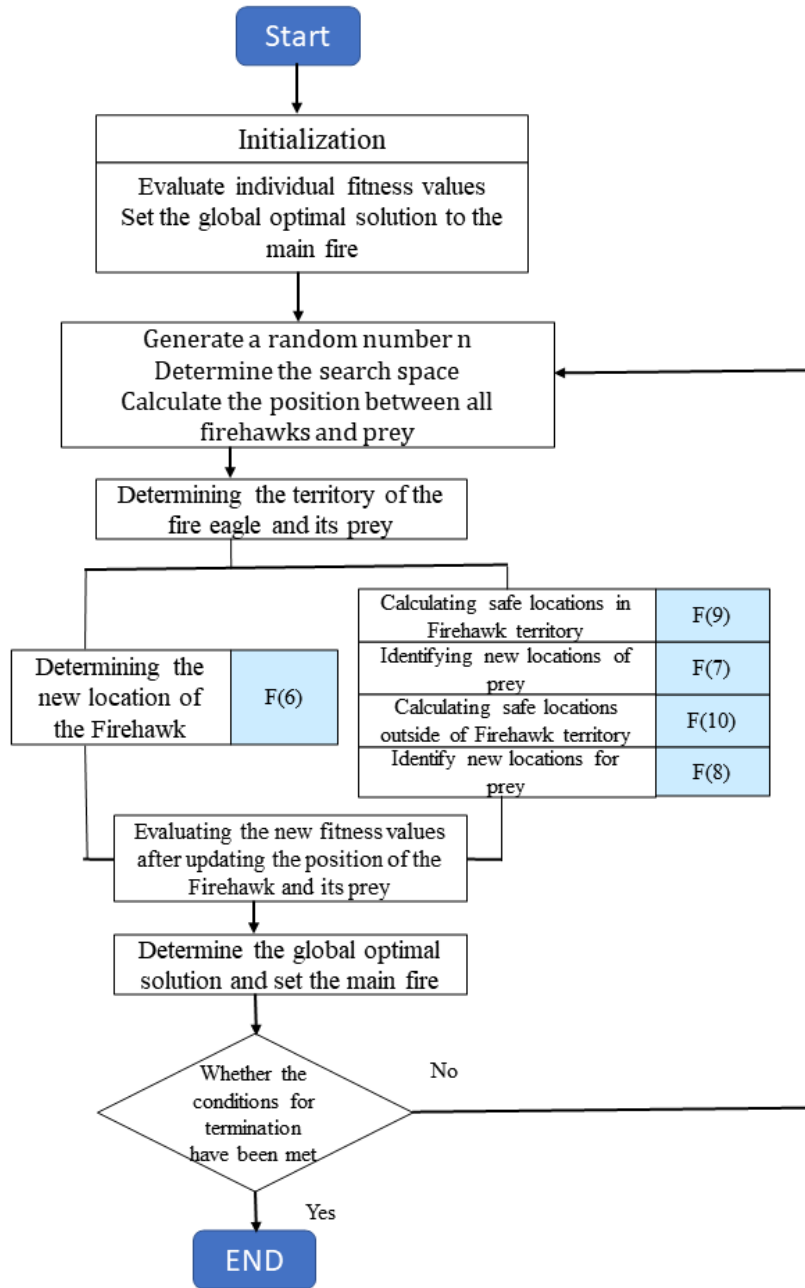


FIGURE 2. The flowchart of an improved firehawk optimization algorithm.

In order to perform a comprehensive experimental test of the FHO, the quality of the FHO was assessed by using a set of classical functions [36]. This set of functions is divided into two categories: the first category is called single-peaked functions, and the main feature that discriminates these functions is that they have only one extreme value point in the search domain, as shown in Table 1. The second category is called multi-peaked functions, which have more than one locally optimal extreme value point in a certain range, as shown in Table 2.

TABLE 1. Six test functions with a single peak.

Function	Description	Dimension	Range	Optimum
F1	$f(x) = \sum_{i=1}^n x_i^2$	30	[-100,100]	0
F2	$f(x) = \sum_{i=0}^n  x_i  + \prod_{i=0}^n  x_i $	30	[-10,10]	0
F3	$f(x) = \sum_{i=1}^d (\sum_{j=1}^i x_j)^2$	30	[-100,100]	0
F5	$f(x) = \sum_{i=1}^{n-1} [100(x_i^2 - x_{i+1})^2 + (1 - x_i)^2]$	30	[-30,30]	0
F6	$f(x) = \sum_{i=1}^n ([x_i + 0.5])^2$	30	[-100,100]	0
F7	$f(x) = \sum_{i=0}^n i x_i^4 + \text{random } [0,1)$	30	[-1.28,1.28]	0

TABLE 2. Three test functions with multiple peaks.

Function	Description	Dimension	Range	Optimum
F8	$f(x) = \sum_{i=1}^n (-x_i \sin(\sqrt{ x_i }))$	30	[-500,500]	-418.9829
F10	$f(x) = -20 \exp\left(-0.2 \sqrt{1/n \sum_{i=1}^n x_i^2}\right) - \exp(1/n \sum_{i=1}^n \cos(2\pi x_i)) + 20 + e \sum_{i=1}^{n-1} (y_i - 1)^2 [1 + 10 \sin^2(\pi y_{i+1}) + \sum_{i=1}^n u(x_i, 10, 100, 4)],$ where $y_i = 1 + \frac{x_i+1}{4}, u(x_i, a, k, m) \begin{cases} K(x_i - a)^m & \text{if } x_i > a \\ 0 & -a \leq x_i \leq a \\ K(-x_i - a)^m & -a \leq x_i \end{cases}$	30	[-32,32]	0
F12	$f(x) = \sum_{i=1}^n (-x_i \sin(\sqrt{ x_i }))$	30	[-50,50]	0

We have selected some other algorithms for comparison experiments with FHO, such as PSO, GWO and WHO algorithms. From these results, it can be obtained that FHO achieved good results in most of the above function tests, as shown in Table 3. We have selected a graph of the iterative process for some of the functions, as shown in Figure 3. Among them, it can be clearly seen that the search speed and seek quality of the FHO algorithm is excellent. This reflects that the performance of FHO is more advantageous. Therefore, the initial parameters of the neural network algorithm were searched for superiority using FHO in the next experiments.

From these results, it can be obtained that FHO achieved good results in most of the above function tests, as shown in Table 3. We have selected a graph of the iterative process for some of the functions, as shown in Figure 3. Among them, it can be clearly seen that the search speed and seek quality of the FHO algorithm is excellent. This reflects that the performance of FHO is more advantageous. Therefore, the initial parameters of the neural network algorithm were searched for superiority using FHO in the following numerical experiments.

#### 4. The experimental setup and results.

**4.1. Experimental environment.** All models in this chapter were implemented using the python programming language, and the RNN, LSTM and GRU based electricity load forecasting models were implemented using the keras deep learning library. The hardware environment for the above training models was an IntelCorei5-1035G1 CPU with 16GB of memory.

**4.2. Data sources.** The experimental data for area A in this paper are provided from the publicly available dataset in the 9th Electrical Mathematical Modelling Competition [37], where those numerical data were collected for the period between Year 2012 and

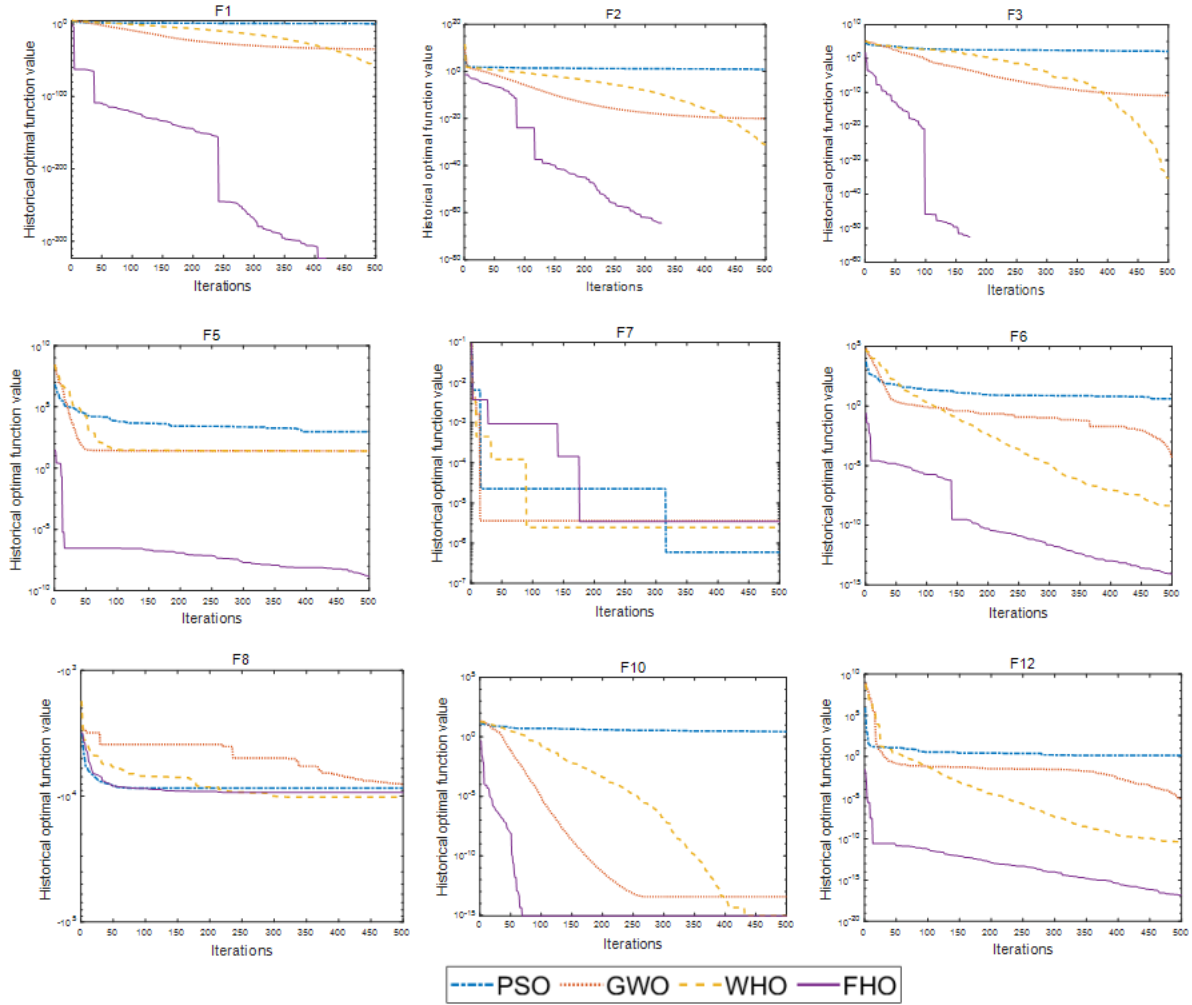


FIGURE 3. The trend comparisons of four optimization algorithms on nine test functions.

Year 2015. The studied dataset was sampled for a one-day period and the corresponding meteorological data, including features such as temperature, humidity and rainfall, were downloaded to predict the short-term load. The paper proposes to train the first 80% of the dataset and use the second 20% of the dataset as a test set for model prediction.

**4.3. Data processing.** Experimental data processing is a very important step in data analysis. If the data is not normalized, the quantity difference between each feature is too large, which makes the model difficult to converge in the training process, Resulting in large errors. In order to avoid too large drop of data values during model training, which will cause too large error in the model, all data shall be normalized first, and then their values shall be compressed between 0 and 1. Therefore, we have the following formula:

$$y = \frac{x - \min(x)}{\max(x) - \min(x)}. \tag{11}$$

**4.4. Long short-term memory neural network.** The LSTM neural network model controls the long-term state through three gates [14, 15] . In Figure 4, it shows the structure diagram of LSTM neural network model, in which LSTM model has three input values and two output values, including the input value at time epoch  $t$ , the output value

TABLE 3. The performance evaluation of four optimization algorithms on thirteen test functions.

Function	Indicators	PSO	GWO	WHO	FHO
F1	Opt.	3.86E+00	2.95E-35	3.64E-59	0.00E+00
	Avg.	6.75E+00	1.55E-33	2.85E-48	<b>6.74E-149</b>
	Std.	1.75E+00	2.48E-33	1.56E-47	3.30E-148
F2	Opt.	7.90E+00	1.12E-20	8.03E-32	0.00E+00
	Avg.	1.89E+01	6.50E-20	2.68E-28	<b>1.03E-67</b>
	Std.	9.98E+00	5.53E-20	7.75E-28	5.65E-67
F3	Opt.	1.25E+02	1.18E-11	3.24E-36	0.00E+00
	Avg.	1.87E+02	6.49E-08	1.86E-28	<b>3.74E-92</b>
	Std.	5.03E+01	1.66E-07	7.02E-28	1.67E-91
F5	Opt.	9.41E+02	2.52E+01	2.49E+01	1.46E-09
	Avg.	2.17E+03	2.69E+01	2.56E+01	<b>1.24E-05</b>
	Std.	1.02E+03	8.94E-01	3.59E-01	1.81E-05
F6	Opt.	4.12E+00	4.19E-05	4.39E-09	8.40E-15
	Avg.	6.86E+00	5.18E-01	8.31E-07	<b>2.66E-11</b>
	Std.	1.95E+00	2.79E-01	2.01E-06	4.91E-11
F7	Opt.	5.92E-07	3.60E-06	2.46E-06	3.46E-06
	Avg.	2.31E-04	4.91E-05	4.49E-05	<b>3.75E-05</b>
	Std.	2.10E-04	4.67E-05	5.64E-05	3.54E-05
F8	Opt.	-8.62E+03	-7.99E+03	-1.02E+04	-9.33E+03
	Avg.	-7.10E+03	-6.15E+03	<b>-9.24E+03</b>	-8.33E+03
	Std.	8.34E+02	9.74E+02	4.07E+02	5.40E+02
F10	Opt.	2.70E+00	3.64E-14	8.88E-16	8.88E-16
	Avg.	3.98E+00	4.39E-14	1.13E-15	<b>8.88E-16</b>
	Std.	4.45E-01	5.78E-15	9.01E-16	0.00E+00
F12	Opt.	1.32E+00	4.91E-06	4.38E-11	1.54E-17
	Avg.	5.34E+00	2.72E-02	3.46E-02	<b>7.88E-12</b>
	Std.	2.63E+00	1.75E-02	1.20E-01	2.91E-11

at time epoch  $t1$ , and the unit state at time epoch  $t1$ . The output includes LSTM output value at the current time and unit state at the current time [19, 20].

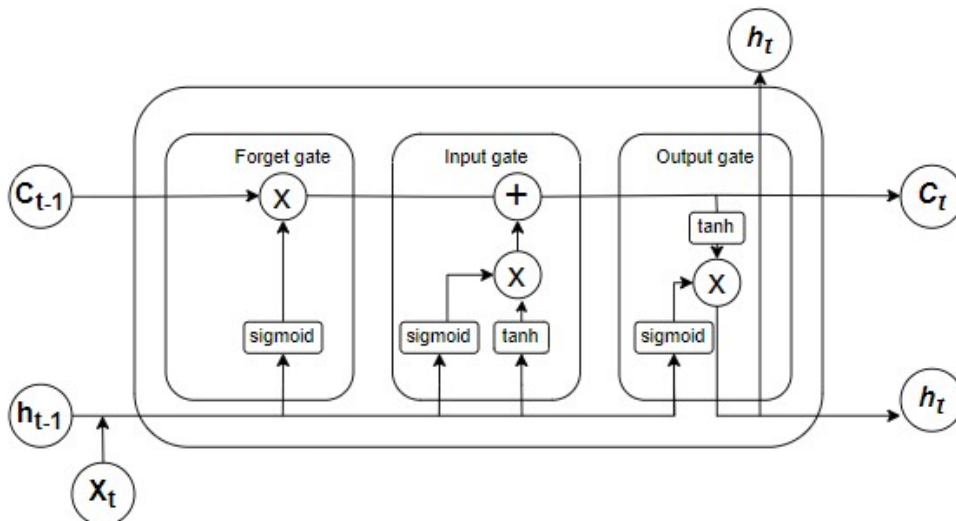


FIGURE 4. The structure diagram of studied LSTM neural network.

The switch mentioned above is called a gate. Let  $W$  be the weight vector of the gate and  $b$  be the threshold. Its function is to make the model output a vector between 0 and 1 times the vector to be controlled. When the gate outputs a zero vector, it means

TABLE 4. The parameters settings for two compared models.

Model	Nue1	Nue2	Dropout	Batch Size	Learning Rate	Patience	n_past
LSTM	44	23	0.00834	15	0.01	25	14
FHO LSTM	32	66	0.46614	39	0.01	35	14

that no information can pass through. When the gate outputs 1 vector, it means that any information can pass through. According to the above description of LSTM, the forward algorithm of LSTM neural network is mainly to update and output the cell state, forgetting gate, output gate and inputs mentioned above. The calculation formula is:

$$f_t = \sigma(\omega_f[h_{t-1}, X_t] + b_f), \tag{12}$$

$$i_t = \sigma(\omega_i[h_{t-1}, X_t] + b_i), \tag{13}$$

$$\tilde{C}_t = \tanh(\omega_C[h_{t-1}, X_t] + b_C), \tag{14}$$

$$O_t = \sigma(\omega_o[h_{t-1}, X_t] + b_o), \tag{15}$$

$$h_t = O_t * \tanh(C_t). \tag{16}$$

**4.5. Evaluation indicators.** The logical regression model is mainly used to evaluate the difference between the predicted value and the true value to judge whether the model is good or not. In this paper, we select the Mean Square Error (MSE) and the Mean Absolute Variance (MAE) to evaluate the performance of the studied models. Assume that  $N_s$  is the sample size,  $y_i$  is the real value of the sample at time  $i$ , and  $\hat{y}_i$  is the predicted value of the sample.

a. Mean Square Error (MSE): The MSE is a convenient method to measure the average error. The smaller the MSE, the higher the prediction accuracy. The calculation formula is expressed as follows:

$$MSE = \frac{SSE}{N} = \frac{1}{N} \sum_{I=1}^N (y_i - \hat{y}_i)^2. \tag{17}$$

b. Mean Absolute Variance (MAE): The smaller the MAE, the higher the prediction accuracy. The calculation formula is expressed as follows:

$$MAE = \frac{1}{N} \sum_{i=1}^N |y_i - \hat{y}_i|. \tag{18}$$

**4.6. The parameter settings in numerical experiments.** The parameters of the neural network model in this chapter are set as shown in Table 4 below, and the parameters such as the number of hidden layers and neurons are obtained by the FHO optimization algorithm.

**4.7. The improved hybrid neural network based on FHO algorithm.** In general, simple prediction algorithms are low in complexity and fast in prediction, but not effective, while hybrid models can significantly improve the accuracy of the algorithm. We selected MSE from the two judging metrics as the optimization target of the optimization algorithm, and optimization was sought for the four parameters of Nue1, Nue2, Dropout, batch-size in the neural network. The simple algorithm steps of the hybrid model proposed in this chapter are as follows, its flowchart is shown in Figure 5. (1) FHO search for optimal parameters: The FHO metaheuristic algorithm simulates the foraging behavior of the firehawk and performs the search and selection of the global optimal solution. (2) Prediction: The clustered data are normalized to load data and then input to set the optimal parameters for the FHO search for load prediction.

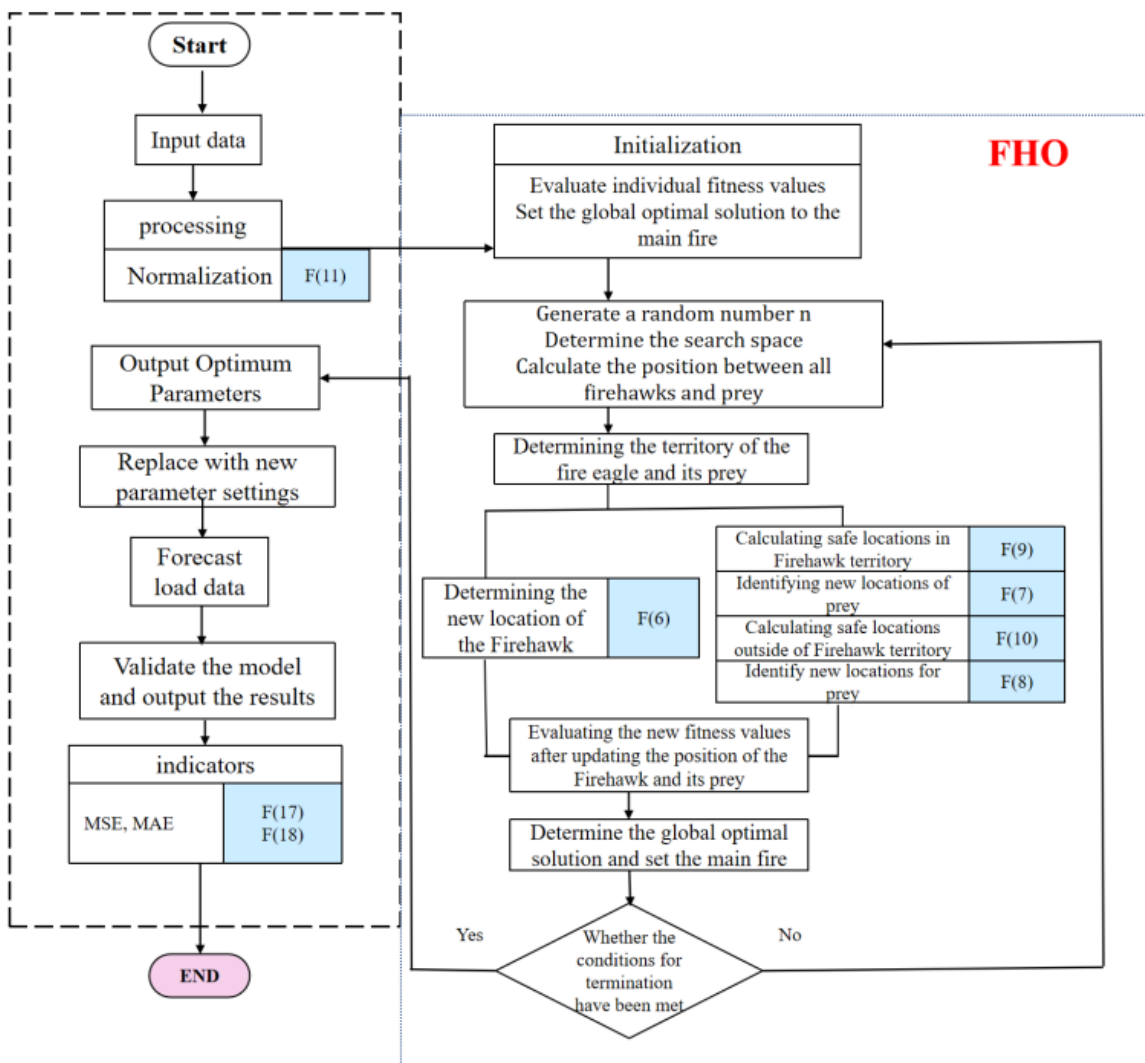


FIGURE 5. The flowchart of our hybrid neural network based on fire hawk optimization algorithm.

**4.8. Numerical results.** From the experimental simulation results, Table 5 clearly shows the data plots of the judging indicators for the results of each experimental model in areas A and B. it can be seen that Taking the results of region A as an example, the MSE of the

improved LSTM neural network was reduced by 0.0027. The MAE of the improved LSTM neural network has been reduced by 0.011. In Figure 7, it shows the prediction graph of FHO-LSTM, and Figure 6 shows the prediction graph of LSTM. From the comparison of simulation results, The prediction results of FHO-LSTM are more accurate. After comparing the simulation experiments, the improved LSTM prediction method based on FHO is more accurate compared to the LSTM prediction model. It is clear from the performance judging table that the load prediction values of the improved prediction model based on the combination of FHO and neural network proposed in this paper are more accurate, indicating the effectiveness of the improved prediction model proposed in this paper.

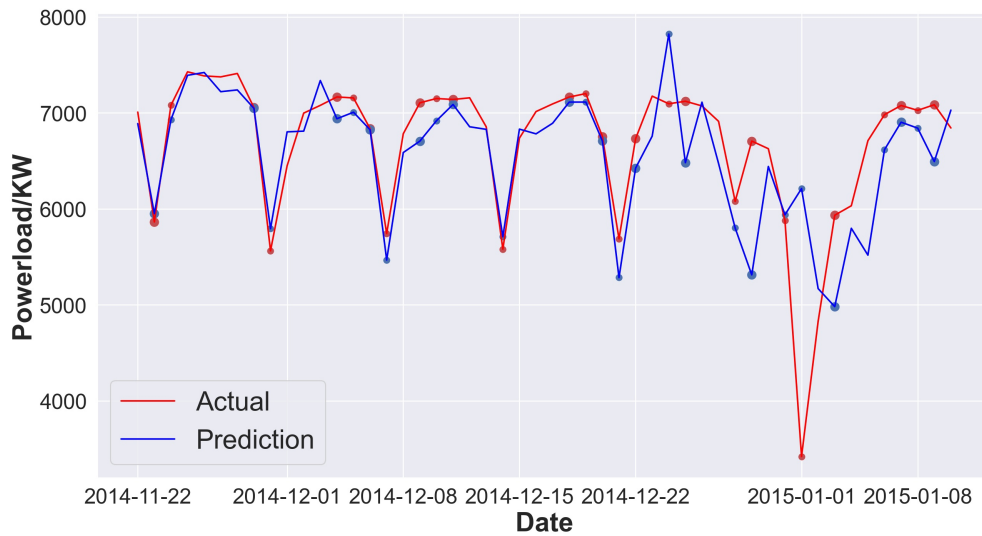


FIGURE 6. LSTM load forecasts for region A.

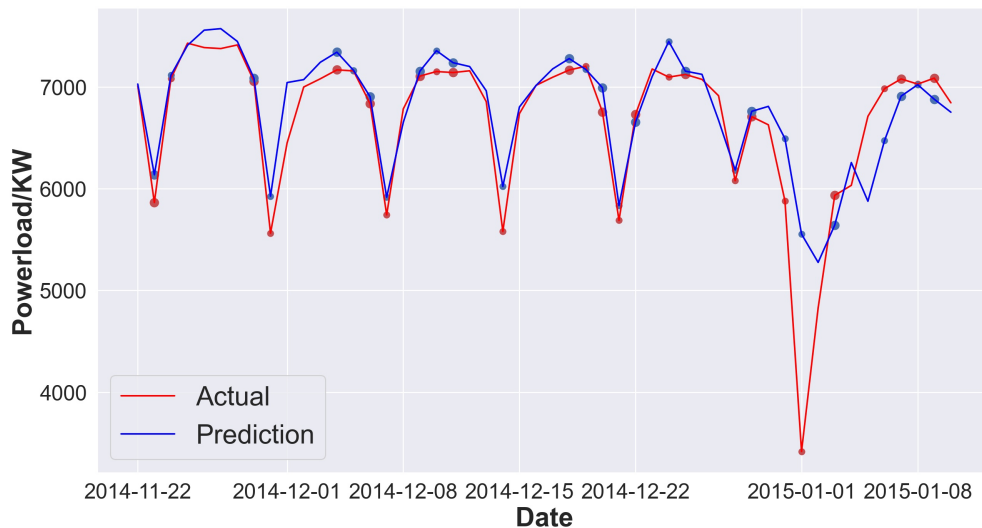


FIGURE 7. FHO-LSTM load forecasts for region A.

**5. A decision-making process for economic load dispatch problem in electric power system.** In the previous section, it has been verified the high accuracy of forecasting the short-term loads based on the presented hybrid neural network, which is going

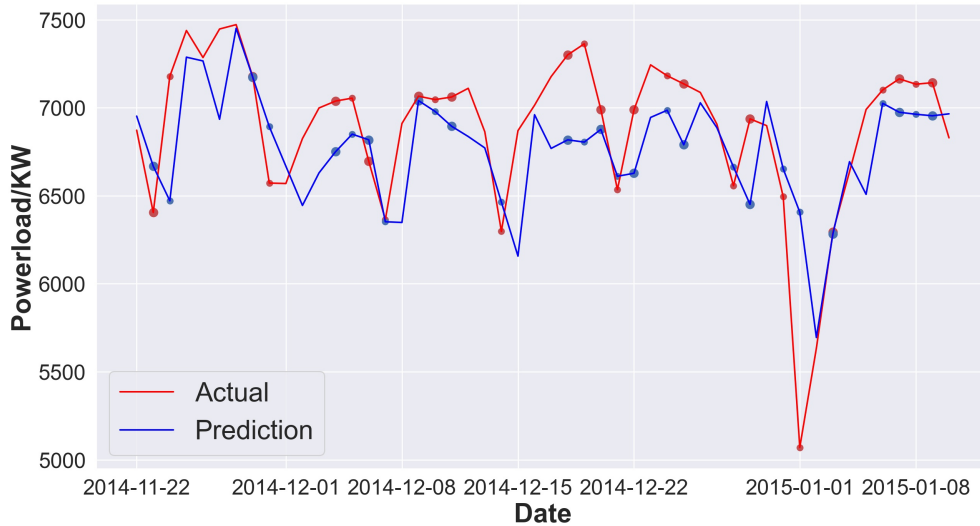


FIGURE 8. LSTM load forecasts for region B.

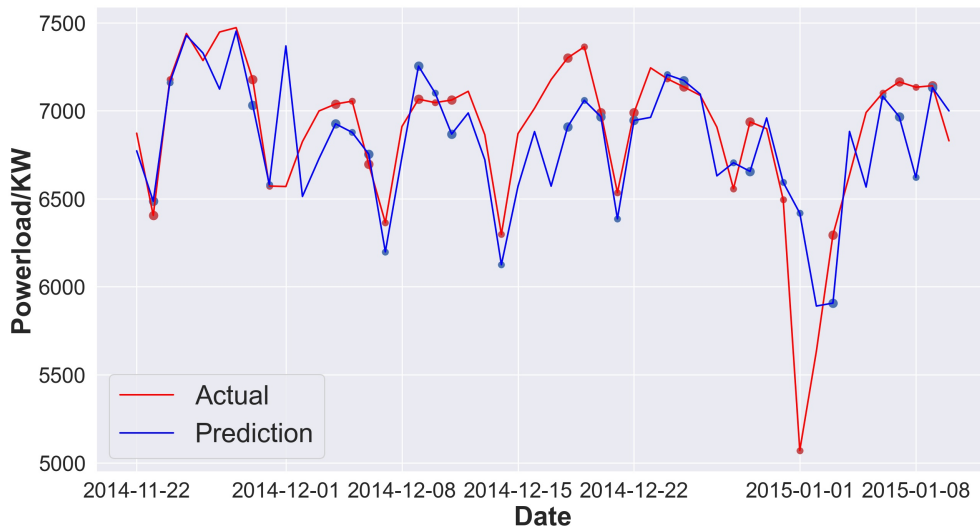


FIGURE 9. FHO-LSTM load forecasts for region B.

TABLE 5. Evaluation indicators for two models in comparison experiments of areas A and B.

MODEL	MSE(A)	MAE(A)	MSE(B)	MAE(B)
LSTM	0.0078	0.0548	0.0058	0.0539
FHO LSTM	<b>0.0051</b>	<b>0.0438</b>	<b>0.0052</b>	<b>0.0531</b>

to provide an effective basis for conducting a better economic dispatch decision. This helps to develop more scientifically efficient economic dispatch decisions, thus ensuring the safe operation of the power system. In the field of power system planning and operation, optimizing the economic operation of power systems is a very important topic. In economic dispatch decisions, the operating parameters and management of the unit are usually optimized to reduce the unit's operating costs and improve efficiency.

**5.1. An optimization model for economic operation of unit combinations.** In power systems, efficient resource dispatch is essential for the economic operation of the

TABLE 6. The notations in the studied optimization model for economic operation of unit combinations.

Symbol	Instruction
$u_{i,t}$	Start/stop state of unit $i$ at time $t$
$P_{i,t,s}$	Power output of unit $i$ in the $s$ th segment of the segmentation part of time period $t$
$P_{i,t}$	Output of unit $i$ at time $t$
$C_i^f$	Coal consumption cost of unit $i$
$C_i^u$	Start-up costs of unit $i$
$C_i^D$	Shutdown costs of unit $i$
$a_i, b_i, c_i$	Coal consumption factor for unit $i$
$P_{d,t}$	Load demand at node $d$ in time slot $t$
$P_{i,max}, P_{i,min}$	Maximum and minimum output limits for unit $i$
$P_{1,max}, P_{1,min}$	Tidal current constraint for line 1 (bi-directional)
$\rho$	Thermal reserve factor
$R_d, R_u$	Down/up climb rate of the unit
$TS, TO$	Minimum off/on time
$H_i, J_i$	Single start-up/shutdown cost of unit $i$

power system. Therefore, the supply and demand balance of the power system is ensured, and the supply-side benefits are maximized, i.e., the operating costs of the units are reduced. The objective of the Unit Commitment (UC) optimization problem is to minimize the total operating cost of a generating unit, given the start-stop state and real-time power output of the unit, and to meet certain technical safety constraints, including generator output constraints, start-stop time constraints and power balance constraints. The supply-side costs can be reduced by controlling the number of starts and stops and optimizing the power allocation of the units. In Table 6, we summarize the mathematical notations in the studied optimization model for economic operation of unit combination.

The objective function is the minimization of the total cost [24], which includes the cost of coal consumption due to power generation and the start-up and shut-down costs arising from the start-up and shut-down of the unit. By using the load forecast data as the load constraint for unit at time , the equation is as follows:

$$\min \sum_{i=1}^N \left( \sum_{t=1}^T C_i^f(P_{i,t}) + C_i^U + C_i^D \right), \quad (19)$$

where the coal consumption function of the unit is formulated as

$$c_i(P_{i,t}) = a_i P_{i,t}^2 + b_i P_{i,t} + c_i. \quad (20)$$

(1) Equation constraint:

$$\sum_{i=1}^N P_{i,t} = \sum_{i=1}^{N_L} P_{d,t}, \quad (21)$$

(2) Inequality constraint:

i. Hot standby:

$$\sum_{i=1}^N (u_{i,t} P_{i,max} - P_{i,t}) \geq \rho \sum_{i=1}^{N_L} P_{d,t}, \quad (22)$$

ii. Unit output constraints:

$$P_{i,\min} \leq P_i \leq u_{i,t} P_{i,\max}, \quad (23)$$

iii. Unit climbing constraints:

$$-R_d \leq P_{i,t} - P_{i,t-1} \leq R_u, \quad (24)$$

iv. Unit start/stop time constraint:

$$\sum_{k=t}^{t+TS-1} (1 - u_{i,k}) \geq TS(u_{i,t-1} - u_{i,t}), \quad (25)$$

$$\sum_{k=t}^{t+TS-1} u_{i,k} \geq TO(u_{i,t} - u_{i,t-1}), \quad (26)$$

v. Start-stop cost constraint:

$$C_{i,t}^U \geq H_i(u_{i,t} - u_{i,t-1}), C_{i,t}^U \geq 0, \quad (27)$$

vi. Trendy safety restraints:

$$P_{l,\min} \leq P_{l,t} \leq P_{l,\max}. \quad (28)$$

**5.2. The simulation analysis of economic load dispatch decisions.** In this section, the experimental results of the FHO-LSTM model are going to be selected as the constraints for the simulation experiments, combined with the experimental results in Section 3. Here, we apply the classical IEEE30 test system [25] to verify the comparative analysis of the effect of the FHO-LSTM short-term prediction model proposed in this paper on the reduction of power system operating costs. The system wiring diagram is shown in Figure 10, and the system contains thirty nodes with six generating units. The purpose of the numerical experiments in this subsection is to reasonably determine the optimal combination of units in the system based on the load forecasting results determined by the proposed FHO-based hybrid neural networks (shown as Figure 11), to achieve the effect of reducing the operating cost of the power system.

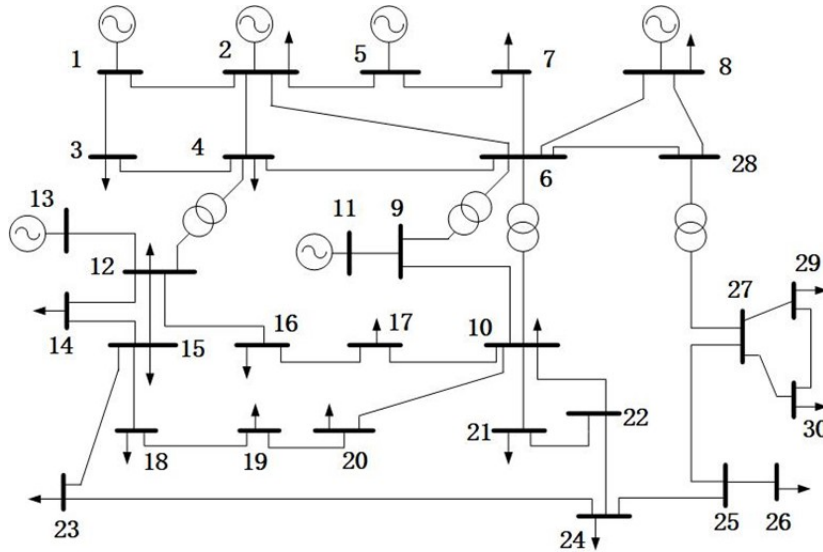


FIGURE 10. An illustrative example of the IEEE30 node test system.

TABLE 7. The parameter settings for the simulated power system with six generating units.

Unit	Node	$P_{max}$	$P_{min}$	$a_i$	$b_i$	$c_i$	Ru/Rd	TS/TO	$H_i$	$J_i$
1	1	1.5749	0.5	0.1524	38.5397	786.7988	0.375	2	39372.5	19686.25
2	2	1	0.25	0.1058	46.1591	945.6332	0.3	2	25000	12500
3	5	0.6	0.15	0.028	40.3965	1049.998	0.15	2	15000	7500
4	8	0.8	0.2	0.0354	38.3055	1243.531	0.2	2	20000	10000
5	11	0.4	0.1	0.0211	36.3278	1658.57	0.15	2	10000	5000
6	13	0.4	0.1	0.0179	38.2704	1356.659	0.15	2	10000	5000

In Table 7, it summarizes the parameter settings for the simulation system with six generating units and thirty nodes. The units of and are p.u., and the notations , and denote coal consumption coefficients in tons/p.u., tons/p.u. and tons, respectively. The symbol Ru/Rd denotes the climbing rate of the unit in p.u./hour, and the symbol TS/TO denotes the minimum start-up and shutdown time in hour. The notations and indicate the cost (in \$/stop) of a single start and stop of the unit, respectively. The data are based on the standardized system, so the power parameters and network parameters are also standardized and dimensionless.

As an illustrated example of the economic dispatch optimization scheme, we conduct the power load forecasting, dispatch decisions, and economic efficiency analysis in the following. Firstly, the numerical results for the power load forecasting are shown in Figure 11, which depicts the hourly load prediction results for a specific date (January 5, 2015) in the data set. We select the load data collected from January 1 to January 4, 2015 as the training set in the comparison experiments for two forecasting methods LSTM and FHO-LSTM. Note that, in Figure 11, the prediction results of LSTM are shown on the left side, and the prediction results of FHO-LSTM are shown on the right side. In Table 8, it shows the comparison results of forecasting errors between the LSTM and FHO-LSTM forecasting methods. From the values of the two evaluation indicators, it can be seen that the MSE of the improved LSTM neural network was reduced by 0.0052. The MAE of the improved LSTM has been reduced by 0.0392.

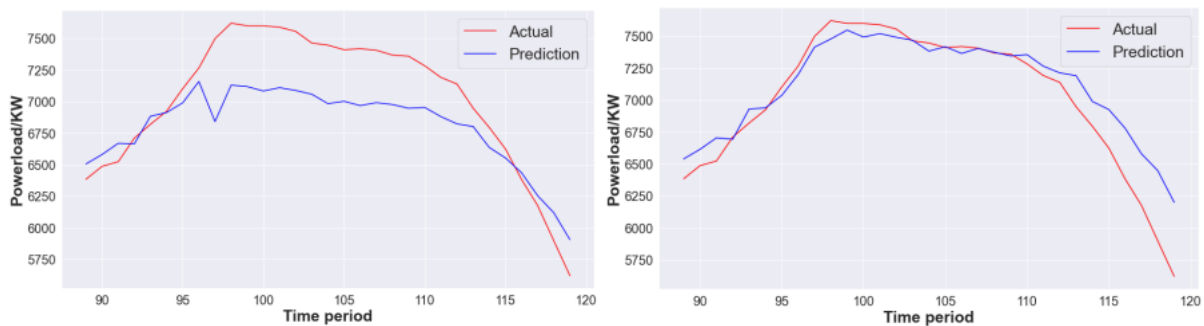


FIGURE 11. The power load forecasting curves based on LSTM (on left side) and FHO-LSTM (on right side) for January 5, 2015.

Next, for determining the dispatch decisions, the power load predicted by our forecasting method for each specific time period will be inputted into the IEEE30 simulation system as the load value for that time period. In Figure 12, it shows the simulation results of the power output of each unit. Besides, the optimized start/stop plan for six units is summarized in Table 9. For the unit combination strategy, the power output of each unit for the unit active output scheme is given in Table 10. In Table 9, it indicates the starting

TABLE 8. The comparison results between the LSTM and FHO-LSTM forecasting methods, where bold font represents better results.

MODEL	MSE	MAE
LSTM	0.0084	0.0773
<b>FHO LSTM</b>	<b>0.0032</b>	<b>0.0381</b>

TABLE 9. The optimized start/stop scheme for units.

Time period \ Unit	1	2	3	4	5	6
1	1	1	0	0	0	0
2	1	1	0	0	0	0
3	1	1	0	0	0	0
4	1	1	0	0	0	0
5	1	1	0	0	0	0
6	1	1	0	0	0	0
7	1	1	1	0	0	0
8	1	1	1	0	0	0
9	1	1	0	1	0	0
10	1	1	1	1	0	0
11	1	1	1	1	0	0
12	1	1	1	1	0	0
13	1	1	1	1	0	0
14	1	1	1	1	0	0
15	1	1	1	1	0	0
16	1	1	1	1	0	0
17	1	1	1	1	0	0
18	1	1	1	1	0	0
19	1	1	1	1	0	0
20	1	1	0	1	0	0
21	1	1	0	1	0	0
22	1	1	1	0	0	0
23	1	1	1	0	0	0
24	1	1	0	0	0	0

and stopping status of the units at each time, with 0 indicating stop and 1 indicating start. In Table 10, it shows the output of each unit at each time. From the empirical analysis in Table 9, it can be observed that units 1 and 2 are in start-up operation during the day. Besides, as the load demand increases, units 3 and 4 are started and put into operation one after another. When the load demand changes, the optimal combination of units and output is selected by weighing the cost of generation against the start-up and shut-down costs.

Finally, in order to analyze the economic efficiency of corresponding dispatch strategies, we compare the operating costs of the power system under the studied economic dispatch model. The final unit operating costs are given in Table 11. The effectiveness of the improved model proposed in this paper, by improving the accuracy of load forecasting, can achieve a reduction in operating costs, thus maximizing the supply and demand side benefits.

The short-term power load forecasting results presented in this paper can be further developed and used to optimize the combination of power units in such a way that the

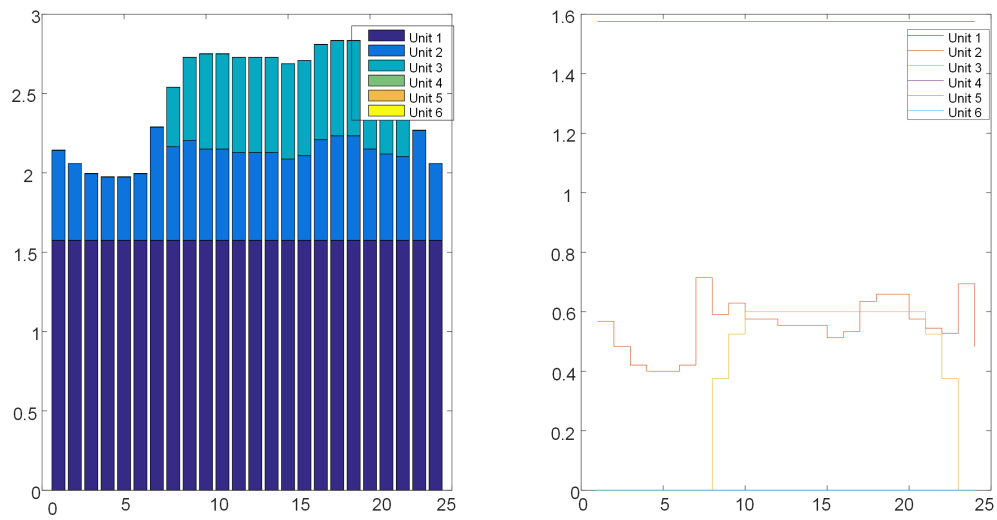


FIGURE 12. The simulation results of the power output of each unit.

TABLE 10. The power output of each unit.

Time period \ Unit	1	2	3	4	5	6
1	1.5749	0.567970632	0	0	0	0
2	1.5749	0.483704589	0	0	0	0
3	1.5749	0.420874648	0	0	0	0
4	1.5749	0.400177725	0	0	0	0
5	1.5749	0.400177725	0	0	0	0
6	1.5749	0.420874648	0	0	0	0
7	1.5749	0.339327438	0.375	0	0	0
8	1.5749	0.59064721	0.375	0	0	0
9	1.5749	0.654137037	0	0.5	0	0
10	1.5749	0.475573135	0	0.7	0	0
11	1.5749	0.375573135	0	0.8	0	0
12	1.5749	0.354137037	0	0.8	0	0
13	1.5749	0.354137037	0	0.8	0	0
14	1.5749	0.354137037	0	0.8	0	0
15	1.5749	0.312743194	0	0.8	0	0
16	1.5749	0.333440114	0	0.8	0	0
17	1.5749	0.434707198	0	0.8	0	0
18	1.5749	0.25	0.2091	0.8	0	0
19	1.5749	0.25	0.2091	0.8	0	0
20	1.5749	0.475573135	0	0.7	0	0
21	1.5749	0.569870997	0	0.5	0	0
22	1.5749	0.527817265	0.375	0	0	0
23	1.5749	0.318630518	0.375	0	0	0
24	1.5749	0.483704589	0	0	0	0

supply and demand sides of the power system achieve a dynamic balance and maximize the overall benefits.

TABLE 11. The determined running costs for two compared methods in the studied system.

Method	System running costs (\$)
LSTM based scheduling scheme	6,975,152.00
FHO LSTM based scheduling scheme	6,024,700.00

**6. Conclusions.** The development of the electricity market in China is a process that requires continuous improvement. With the increase in electricity consumption and the need for renewable energy to enter the grid, the development of smart grids faces great challenges. In this paper, aiming to improve the operational efficiency of the power systems in China, we studied an improved load forecasting method, which combines a hybrid neural network with the FHO algorithm. In this work, we implemented a hybrid FHO-based neural network to improve short-term load forecasting, where the FHO algorithm was introduced to tackle the computational complexity in finding the optimal model parameters. Based on a given load dataset, we conducted a comparison between the proposed method with other commonly used algorithms. It was found that the improved FHO-based algorithm presented in this paper could meet a higher search speed and a larger search volume than other optimization algorithms, such as particle swarm optimization, grey wolf optimizer, and wild horse optimizer. In addition, we developed hybrid prediction models, named FHO-LSTM, and it is also compared with the original method LSTM in the numerical experiments to verify the effectiveness. Based on the comparison results, it illustrated that the proposed method achieved a better effect on the power load prediction, especially in the cases of larger influence on external factors or load data fluctuations. Moreover, based on the load forecasting results, we also conducted an optimization of short-term economic dispatching decisions for power systems in this paper. Combined with the load forecasting results, we determined an optimal dispatching scheme for the combination of supply-side units, which minimized the system operating costs under several practical constraints, including generator output constraints, start-stop time constraints and power balance constraints. In the future works, we could make efforts in the direction of improving the prediction effect and the running time of the presented model. For example, there are still many influencing factors that have not been considered in the prediction model, such as the socio-economic impact and the impact of population settlement. Besides, the weight optimization of the proposed neural network could be further investigated by applying other intelligent optimization algorithms, such as fuzzy-based methods [26], chaotic sparrow search algorithm [27], whale optimization algorithm [28], wolf pack algorithm [29], genetic algorithm [30], and so on.

**Acknowledgments.** This work was supported by Fujian Provincial Department of Science and Technology under Grant No. 2021J011070, and Fujian University of Technology under Grant No. GY-Z18148.

## REFERENCES

- [1] C.-H. Wang, C.-J. Lee, and X.-J. Wu, "A coverage-based location approach and performance evaluation for the deployment of 5G base stations," *IEEE Access*, vol. 8, pp. 123320-123333, 2020.
- [2] T.-Y. Wu, X.-L. Guo, Y.C. Chen, S. Kumari, C.-M. Chen, "Amassing the Security: An enhanced authentication protocol for drone communications over 5G networks," *Drones*, vol. 6, no. 1, 10, 2022.
- [3] T.-Y. Wu, Y.-Q. Lee, C.-M. Chen, Y. Tian, A. Nabhan, "An enhanced pairing-based authentication scheme for smart grid communications," *Journal of Ambient Intelligence and Humanized Computing*, January 2021. [Online]. Available: <https://doi.org/10.1007/s12652-020-02740-2>

- [4] T.-Y. Wu, F.-F. Kong, Q. Meng, S. Kumari, C.-M. Chen, "Rotating behind security: An enhanced authentication protocol for IoT-enabled devices in distributed cloud computing architecture," *EURASIP Journal on Wireless Communications and Networking*, vol. 2023, 36, 2023.
- [5] H.-Y. Guo, Q.-X. Chen, Q. Xia, "Monthly load forecasting method considering time lag effect of economic factors," *Power Grid Technology*, vol. 40, no. 2, pp. 514-520, 2016.
- [6] X.-Y. Bu, W.-K. Liu, P.-Y. Zhu, "Research on clean energy development and utilization for achieving sustainable development," *Energy and Environmental Protection*, vol. 40, no. 2, pp. 38-42, 2018.
- [7] S.-X. Zhang, B.-Z. Zhao, F.-W. Wang, "Short-term forecasting of electric load under massive data," *China Journal of Electrical Engineering*, vol. 35, no. 1, pp. 37-42, 2015.
- [8] J.-L. Li, L.-T. Tian, X.-K. Lai, "Outlook of power energy storage technology in the context of energy internet," *Power System Automation*, vol. 39, no. 23, pp. 15-25, 2015.
- [9] S.-X. Fan, L.-X. Li, S.-Y. Wang, "Research on the application of artificial intelligence technology in power grid regulation and control," *Power Grid Technology*, vol. 44, no. 2, pp. 401-411, 2020.
- [10] C.-H. Wang, Q.G. Zhao, R. Tian, "Short-term wind power prediction based on a hybrid Markov-based PSO-BP neural network," *Energies*, vol. 16, no. 11, 4282, 2023.
- [11] C.-H. Wang, Q. Ye, J.B. Cai, Y.F. Suo, S.M. Lin, J.C. Yuan, and X.J. Wu, "A novel data-driven integrated detection method for network intrusion classification based on multi-feature imbalanced data," *Journal of Intelligent & Fuzzy Systems*, vol. 46, no. 3, pp. 5893-5910, 2024.
- [12] D. L. Marino, K. Amarasinghe and M. Manic, "Building energy load forecasting using deep neural networks," *IECON 2016 - 42nd Annual Conference of the IEEE Industrial Electronics Society*, Florence, Italy, pp. 7046-7051, 2016.
- [13] Y.-F. Liu, Y.-H. Yang, "Research on short-term power load forecasting based on CNN-LSTM," *Science and Technology Innovation and Application*, vol. 1, pp. 84-85, 2020.
- [14] F.M. Bianchi, E. Maiorino, M.C. Kampffmeyer, A. Rizzi, and R. Jenssen, *Recurrent Neural Networks for Short-Term Load Forecasting: An Overview and Comparative Analysis*, Springer, 2017, DOI:10.1007/978-3-319-70338-1.
- [15] S. Hochreiter, J. Schmidhuber, "Long short-term memory," *Neural Computation*, vol. 9, no. 8, pp. 1735-1780, 1997.
- [16] S.A. Ilic, A.Z. Selakov, S.M. Vukmirovic, "Procedure for creating custom multiple linear regression based short term load forecasting models by using genetic algorithm optimization," *Thermal Science*, vol. 25, no. 1, pp. 679-690, 2021.
- [17] A. Sina, D. Kaur, "Short term load forecasting model based on kernel-support vector regression with social spider optimization algorithm," *Journal of Electrical Engineering and Technology*, vol. 15, no. 1, pp. 393-402, 2020.
- [18] M. Sajjad, Z.A. Khan, A. Ullah, "A novel CNN-GRU-based hybrid approach for short-term residential load forecasting," *IEEE Access*, vol. 814, pp. 3759-3768, 2020.
- [19] C.-H. Wang and C.-J. Lee, "Data analysis of portfolio optimization using artificial neural network in China's stock market," *Proceedings of 2019 IEEE 5th International Conference on Big Data Intelligence and Computing (DATACom 2019)*, pp. 33-38, Kaohsiung, Taiwan, November 18-21, 2019.
- [20] C.-H. Wang, X.J. Wu, and Y.-T. Chen, "An empirical analysis for forecasting stock index based on LSTM neural network," *Proceedings of the 5th International Conference on Electronic Information Technology and Computer Engineering (EITCE2021)*, pp. 636-641, Xiamen, China, October 22-24, 2021.
- [21] S. Kumar, A. Damaraju, A. Kumar, S. Kumari, C.-M. Chen, "LSTM network for transportation mode detection," *Journal of Internet Technology*, vol. 22, no. 4, pp. 891-902, 2021.
- [22] C.-H. Wang, J.B. Cai, Q. Ye, Y.F. Suo, S.M. Lin, J.C. Yuan, "A two-stage convolution network algorithm for predicting traffic speed based on multi-feature attention mechanisms," *Journal of Intelligent & Fuzzy Systems*, vol. 45, no. 3, pp. 5181-5196, 2023.
- [23] C.-H. Wang, J. Yuan, Y. Zeng, and S. Lin, "A deep learning integrated framework for predicting stock index price and fluctuation via singular spectrum analysis and particle swarm optimization," *Applied Intelligence*, vol. 54, pp. 1770-1797, 2024.
- [24] J. Park, Y. Jeong, J. Shin, "An improved particle swarm optimization for nonconvex economic dispatch problems," *IEEE Transactions on Power Systems*, vol. 25, no. 1, pp. 156-166, 2010.
- [25] M. Liu, Q. Wang, Y.-X. Zhao, "Research on economic load dispatching method based on adaptive differential evolutionary algorithm," *Electrical Applications Application*, vol. 41, no. 02, pp. 64-69, 2022.

- [26] D.M. Teferra, M.H. Ngoo, and G. Nyakoe, “Fuzzy-based prediction of solar PV and wind power generation for microgrid modeling using particle swarm optimization,” *Heliyon*, vol. 9, no. 1, E12802, January 2023.
- [27] Q.P. Yang, C.-H. Wang, T.-K. Dao, T.-T. Nguyen, Q.G. Zhao, S.M. Chen, “An optimal wind turbine control based on improved chaotic sparrow search algorithm with normal cloud model,” *Journal of Network Intelligence*, vol. 9, no. 1, pp. 108-125, 2024.
- [28] C.-H. Wang, S.M. Chen, Q.G. Zhao, and Y.F. Suo, “An efficient end-to-end obstacle avoidance path planning algorithm for intelligent vehicles based on improved whale optimization algorithm,” *Mathematics*, vol. 11, no. 8, 1800, 2023.
- [29] S.M. Chen, C.-H. Wang, Z.Y. Dong, Q.G. Zhao, Q.P. Yang, Y. Wei, and G.S. Huang, “Performance evaluation of three intelligent optimization algorithms for obstacle avoidance path planning,” *Proceedings of the 14th International Conference on Genetic and Evolutionary Computing (ICGEC2021)*, Jilin, China, October 21-23, 2021. *Lecture Notes in Electrical Engineering*, vol. 833, pp. 60-69, Springer, Singapore, 2022.
- [30] Z.Y. Dong, C.-H. Wang, Q.G. Zhao, Y. Wei, S.M. Chen, and Q.P. Yang, “A study on intelligent optimization algorithms for capacity allocation of production networks,” *Proceedings of 2021 Chinese Intelligent Systems Conference (CISC2021)*, Fuzhou, China, October 16-17, 2021. *Lecture Notes in Electrical Engineering*, vol. 804, pp. 734-743, Springer, Singapore, 2022.
- [31] T.-Y. Wu, A.-K. Shao, J.-S. Pan, “CTOA: Toward a chaotic-based tumbleweed optimization algorithm,” *Mathematics*, vol. 11, no. 10, 2339, 2023.
- [32] T.-Y. Wu, H.-N. Li, S.-C. Chu, “CPPE: An improved phasmatodea population evolution algorithm with chaotic maps,” *Mathematics*, vol. 11, no. 9, 1977, 2023.
- [33] A. Shaik, M.K. Manoharan, A.K. Pani, R. Avala, C.-M. Chen, “Gaussian mutation–spider monkey optimization (GM-SMO) model for remote sensing scene classification,” *Remote Sensing*, vol. 14, no. 24, 6279, 2022.
- [34] C.-M. Chen, S. Lv, J. Ning, M.-T. Wu, “A genetic algorithm for the waitable time-varying multi-depot green vehicle routing problem,” *Symmetry*, vol. 15, no. 1, 124, 2023.
- [35] A. Mahdi, T. Siamak, H. Amir, “Fire Hawk Optimizer: a novel metaheuristic algorithm,” *Artificial Intelligence Review*, vol. 56, pp. 287-363, 2023.
- [36] P. Suganthan, N. Hansen, J. Liang, K. Deb, Y. Chen, A. Auger, “Problem definitions and evaluation criteria for the CEC 2005 special session on real-parameter optimization,” *Natural Computing*, pp. 341-357, 2005.
- [37] China Electrical Engineering Society Electrical Mathematics Special Committee, 2016 Electrical Mathematical Modeling Competition. [Online]. Available: <http://shumo.neepu.edu.cn>